A STUDY ON THE LOW REYNOLDS NUMBER AIRFOILS FOR THE DESIGN OF THREE DIMENSIONAL WING

K.J. Jung,[1] J. Lee,[2] J.H. Kwon[*2] and I.M. Kang[1]

3차원 날개 설계를 위한 저레이놀즈수 에어포일에 대한 연구

정 경 진,[1] 이 재 훈,[2] 권 장 혁,[*2] 강 인 모[1]

In this study, a generic airfoil designed by the inverse method was evaluated with several candidate airfoils as a first step. Each airfoil was compared with respect to aerodynamic performance to meet the requirement of HALE(high altitude long endurance) aircraft. The second step was to optimize the candidate airfoil using the couple of optimization formulations to down select an optimum airfoil. For the analysis of low Reynolds number 2D flow, Drela's MSES was used. After comparing the aerodynamic results, the best airfoil was chosen to construct the baseline 3D wing. The Navier-Stokes code was used to evaluate the overall aerodynamic performance of designed wing with other wings. The results show that the designed wing has the best performance compared with other wings.

Key Words : 저레이놀즈수 에어포일(Low Reynolds number airfoil), 최적설계(Optimization), 공력 특성(Aerodynamic Characteristics), Navier-Stokes Equations

1. INTRODUCTION

The low Reynolds number flow is known as one of complex phenomena because the laminar flow region exists in the beginning, then the transition followed by the turbulent flow region usually. These days, there are increasing demands for the analysis of the low Reynolds number flow due to the development of HALE aircraft. The detail analysis of this flow requires accurate prediction of a transition point.

Various programs were developed for the analysis and design of low Reynolds number airfoil. Among them, MSES, XFOIL and PROFILE are popular. MSES and XFOIL were developed by Drela. MSES solves streamtube Euler equations, therefore it covers subsonic and transonic flows[1,2,3]. XFOIL uses a panel method, therefore it can only solve subsonic flow[4]. PROFILE was developed by Eppler and it was used in the design of low Reynolds airfoils[5,6]. Drela demonstrated the usefulness of optimization methods in the design of airfoils[7]. He used the unconstrained optimizer for the design of subsonic and transonic airfoils.

In this study, the shapes of low Reynolds number airfoil are optimized using various optimization formulations. Additionally, a wing is constructed with the best performance airfoil and its aerodynamic performances are compared with other ones.

2. AIRFOIL DESIGN GOAL

The primary design parameter for the HALE type airfoil is as follows: Based on the structural and fuel requirements, the thickness ratio to chord should be 15 to 17 percent. According to the flight speed and wing loading, the design lift coefficient should be 1.0. And if there is a need to increase the endurance on the aircraft the airfoil should have low profile drag at C_L = 1.0. The high $C_{L,max}$ is required also. This capability can be used to

1 정회원, 국방과학연구소
2 정회원, 한국과학기술원 항공우주공학과
* Corresponding author, E-mail: jhkwon@kaist.ac.kr

increase endurance by flying slower and one needs a very high C_L to land.

The secondary design parameter is to have low pitching moments due to trim drag and to have low drag at low C_L.

3. AERODYNAMIC ANALYSIS

3.1 TWO DIMENSIONAL FLOW

For the two dimensional flow analysis, MSES is used. It solves the streamtube Euler equations and it can handle compressible flows. The e^n method is used to consider the laminar-turbulent transition.

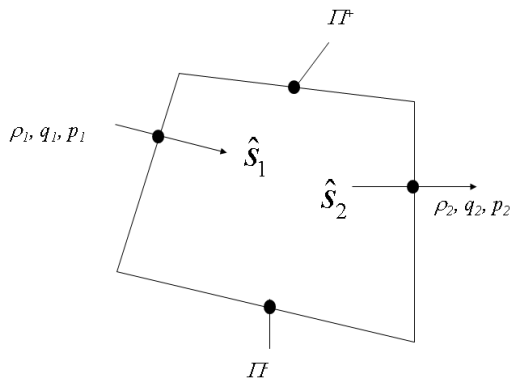

Fig. 1 Streamtube cell and state variables of streamtube Euler equations[3]

Fig. 1 shows a streamtube cell and state variables of streamtube Euler equations[3]. There are density ρ, velocity q and pressure p on each end face which is positioned vertical to streamlines. $\hat{S}$ is the flow vector and its components are p, ρ and q. Π is an average pressure on the streamline faces which are positioned parallel to streamlines. Streamtube Euler equations used in MSES are as follows:

$$\rho_1 q_1 \widehat{S_1} \bullet \overrightarrow{A_1} = \rho_2 q_2 \widehat{S_2} \bullet \overrightarrow{A_2} \tag{1}$$

$$p_1 \overrightarrow{A_1} + \left(\rho_1 q_1 \widehat{S_1} \bullet \overrightarrow{A_1}\right) + \Pi^- \overrightarrow{B^-} = p_2 \overrightarrow{A_2} + \left(\rho_2 q_2 \widehat{S_2} \bullet \overrightarrow{A_2}\right) + \Pi^+ \overrightarrow{B^+} \tag{2}$$

$$H = \frac{\gamma}{\gamma-1}\frac{p_1}{\rho_1} + \frac{1}{2}q_1^2 = \frac{\gamma}{\gamma-1}\frac{p_2}{\rho_2} + \frac{1}{2}q_2^2 \tag{3}$$

$$p_1 + p_2 = \Pi^+ + \Pi^- \tag{4}$$

$\overrightarrow{A}$ is an area vector which is defined along the faces. Eq. (4) is added to constrain for Π to have a reasonable value.

To determine the transition point, an approximate e^n method is used[2]. In this method, the original amplification rate curve is approximated linearly as follows:

$$\overline{n} = \frac{d\tilde{n}}{dRe_\theta}\left[Re_\theta - Re_{\theta,crit}\right] \tag{5}$$

where $\tilde{n}$ means the logarithm of the maximum amplification rate and Re_θ represents the momentum thickness Reynolds number. $d\tilde{n}/dRe_\theta$ and $Re_{\theta,crit}$ can be expressed with empirical formula.

3.2 THREE DIMENSIONAL FLOW

In this study, the Navier-Stokes code named as KFLOW is used and the conservative form of three dimensional compressible Navier-Stokes equations are

$$\frac{\partial q}{\partial t} + \frac{\partial f_i}{\partial x_i} = \frac{\partial f_{vi}}{\partial x_i} \tag{6}$$

where

$$q = \left[\rho, \rho u_1, \rho u_2, \rho u_3, \rho E\right]^T \tag{7}$$

$$f_i = \begin{bmatrix} \rho u_i \\ \rho u_i u_1 + \delta_{i1} p \\ \rho u_i u_2 + \delta_{i2} p \\ \rho u_i u_3 + \delta_{i3} p \\ \rho u_i H \end{bmatrix}, \quad f_{vi} = \begin{bmatrix} 0 \\ \sigma_{ij}\delta_{i1} \\ \sigma_{ij}\delta_{i2} \\ \sigma_{ij}\delta_{i3} \\ u_j \delta_{ij} + k\dfrac{\partial T}{\partial x_i} \end{bmatrix} \tag{8}$$

The quantity ρ, u_1, u_2, u_3, $\boldsymbol{E}$ denote density, pressure, velocity components, and total energy. f_i and f_{vi} are inviscid and viscous fluxes in x, y and z directions respectively. σ_{ij} means the viscous stress. The fluid is assumed to be the air. The pressure is computed from the equation of state and the total energy and total enthalpy $\boldsymbol{H}$ are expressed by its definition:

$$E = \frac{p}{(\gamma-1)\rho} + \frac{1}{2}(u_i u_i) \tag{9}$$

$$H = E + \frac{p}{\rho} \tag{10}$$

The finite volume method is used to discretize the governing equation. For the time integration, DADI(diagonalized alternating direction implicit) is used and the numerical flux is calculated with the upwind TVD(total variation diminishing) and Roe's FDS(flux difference splitting). For the turbulence modeling, the k-ω model is used. Extensive explanation for the numerical methods can be found in references[8,9,10].

4. AERODYNAMIC OPTIMIZATION

Aerodynamic shape optimizations of airfoils are performed. Hicks-Henne functions are used to parameterize the airfoil shape[11]. There are five Hicks-Henne functions on the lower and upper surfaces. Therefore, the total number of design variables are ten. Three optimization formulations are compared and they are as follows:

$$\begin{aligned} &\max C_l \\ &s.t.\ C_d < C_{d0} \\ &\quad C_m > C_{m0} \\ &\quad t > t_0 \end{aligned} \tag{11}$$

$$\begin{aligned} &\max \frac{C_l}{C_d} \\ &s.t.\ C_l > C_{l0} \\ &\quad C_d < C_{d0} \\ &\quad C_m > C_{m0} \\ &\quad t > t_0 \end{aligned} \tag{12}$$

$$\begin{aligned} &\min C_d \\ &s.t.\ C_l > C_{l0} \\ &\quad C_m > C_{m0} \\ &\quad t > t_0 \end{aligned} \tag{13}$$

where t stands for the maximum ratio of thickness to chord and the final constraint of each formulation is inserted to retain t to be greater than a certain value. A constraint concerning the moment is added to prohibit an excessive nose-down pitching moment after aerodynamic shape optimizations.

SQP(sequential quadratic programming) is used as an optimization method[12]. SQP is known as an efficient optimization method for constrained optimization problems requiring less calculation cost than stochastic optimization methods such as the simulated annealing or the evolutionary algorithm.

5. NUMERICAL RESULTS

The low Reynolds number flow around an airfoil is computed with MSES. Three low Reynolds number airfoils are used as initial points of the SQP optimizer. These airfoils are NLF(1)-1015, LRN1015 and a generic airfoil. For each airfoil, three optimization formulations, as in Eq. (11)-(13), are solved with the SQP optimizer. The best performance airfoil is selected among the optimized airfoils, and a wing is constructed using the selected airfoil. The flow around the wing is computed with a Navier-Stokes solver. The analysis result of MS(1)-0317 airfoil which is the 17% thick medium speed airfoil was included for the comparison of optimized airfoils.

5.1 AERODYNAMIC CHARACTERISTICS OF GENERIC AIRFOIL

The profiles given in Table. 1 have been selected from a number of profiles that were investigated. Only the profiles which had a low value of C_d at C_l=1.0 were kept. The candidate airfoils were evaluated in view of aerodynamic performance predicted by XFOIL. A generic airfoil was created from the catalog of existing wing sections having 17% thickness ratio by considering the pressure distribution on the airfoil surface.

The maximum lift for the generic airfoil shows a remarkable improvement over the other airfoils as shown in Fig. 2. The moment coefficients for the airfoils are shown in Fig. 3. The generic airfoil had a low pitching moment coefficient compared with other candidate airfoils. All important drag polars are shown in Fig. 4. It is clear that the LRN1017 exhibits a substantial gain at the design

Table 1 List of several candidate airfoils

Designation	Profile
E583	Eppler's E583 airfoil
FX61-184	Wortman's 17%
LRN1017	LRN1015 with 17% thickness
NACA64187	NACA 6 series of 17% thickness
NLF1017	NLF1015 with 17% thickness
LRN1017o	LRN1017 optimized

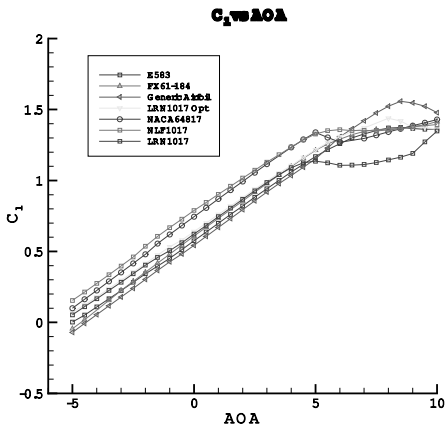

Fig. 2 C_l comparison of various airfoils

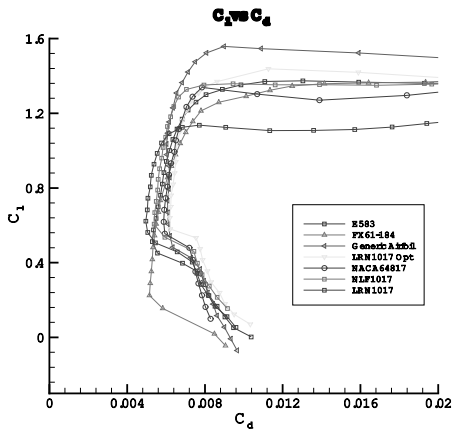

Fig. 4 Drag polar comparison of various airfoils

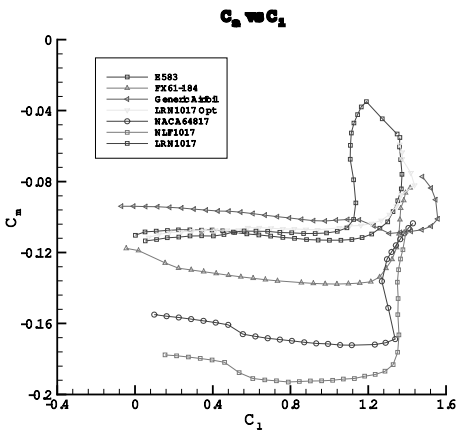

Fig. 3 C_m vs. C_l comparison of various airfoils

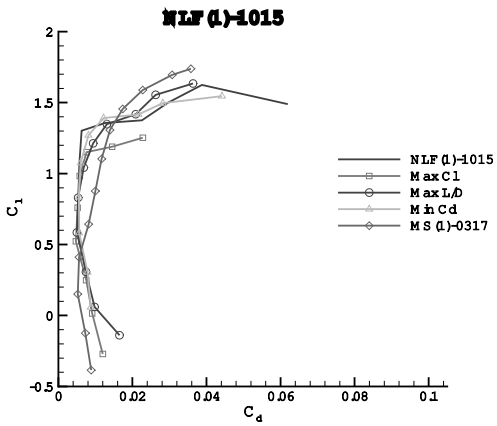

Fig. 5 Drag polar of NLF(1)-1015

C_l, although it does stall earlier than most of other competing profiles. The optimized LRN1017 version shows substantial drag increase. The generic airfoil has the highest C_l , moderate C_m and wider drag polar compared with other airfoils.

5.2 Optimization of Candidate Airfoils

Three airfoils such as NLF(1)-1015, LRN1015, and the generic airfoil were optimized to find out the optimal airfoil shape using the MSES. The following results show the initial and final shapes after optimization and the aerodynamic characteristics were presented to figure out the differences between them.

5.2.1 NLF(1)-1015 Airfoil

This airfoil is designed using Eppler's PROFILE to adapt to the high altitude environment. In the name of the airfoil, NLF means the natural laminar flow[13]. The first two digits after NLF are related with a design lift coefficient which is 1.0 and the last two digits are related with the maximum ratio of thickness to chord which is 0.15.

Fig. 5 shows the results of the aerodynamic optimization. In each figure, Max C_l refers to the result of Eq. (11), Max L/D refers to the result of Eq. (12) and Min C_d refers to the result of Eq. (13). The result of Max C_l shows an excessive increase in the thickness and lower aerodynamic performance with regard to the lift

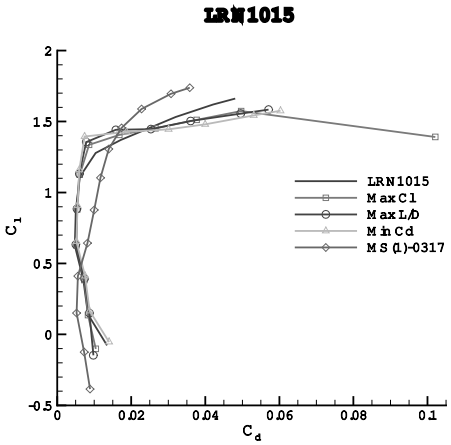

Fig. 6 Drag polar of LRN1015

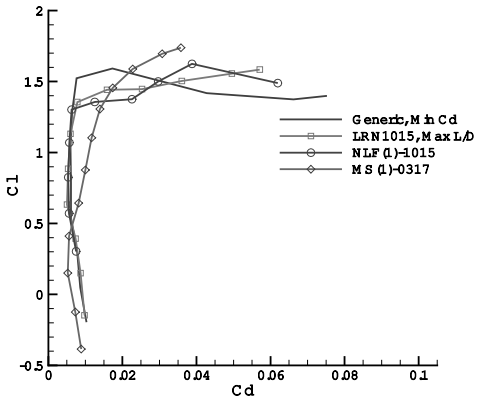

Fig. 8 Drag polar comparison of various airfoil

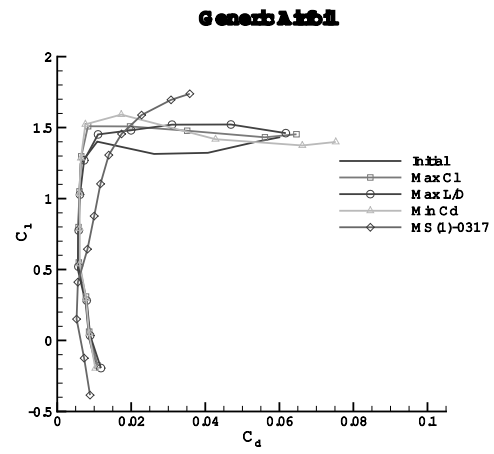

Fig. 7 Drag polar of generic airfoil

than other results. While having the high lift coefficient, NLF(1)-1015 has an excessive pitching moment. It means this airfoil will get some more trim drag than other airfoils.

5.2.2 LRN1015 AIRFOIL

In the name of this airfoil, LRN means the low Reynolds number and first two digits following LRN give the design lift coefficient in tenths; the last two digits indicate the approximate maximum thickness/chord ratio in hundredths[14]. Hence, the design lift coefficient of the LRN1015 airfoil is 1.0 and the maximum thickness/chord ratio is 0.152. The airfoil was designed for a Mach number of 0.55 and a Reynolds number of 500,000 and this airfoil has a long rooftop pressure distribution on the upper surface.

Fig. 6 shows the results of aerodynamic optimization. The Min. C_d case has some gain in C_l = 1.4 compared with original profile. Generally all three optimized cases show good performance and they exhibit extended drag buckets in Fig. 6.

5.2.3 GENERIC AIRFOIL

Fig. 7 shows the results of aerodynamic optimization for the generic airfoil. All the optimized cases gave better aerodynamic performances compared with the initial airfoil. Min C_d case shows the best drag polar as depicted in Fig. 8. The lift over drag ratio of this Min C_d case shows good when the angle of attack equal to 5 or 6 degrees.

5.3 COMPARISON OF AIRFOILS

Among various candidate optimized airfoils, the best airfoils should be selected to meet the requirement of low Reynolds number flow condition. The generic airfoil with Min C_d, LRN1015 with Max L/D and NLF(1)-1015 cases are down selected from the combination of 12 cases and their aerodynamic characteristics are compared in Fig. 8. The generic Min C_d airfoil exhibits the low drag bucket near a point where the lift coefficient is 1.5. Namely, the generic airfoil with Min C_d shows the widest drag bucket. Therefore, this airfoil is chosen as a baseline airfoil for the low Reynolds three-dimensional wing.

5.4 THREE DIMENSIONAL WING

Using the down-selected airfoil, a 3D wing grid was

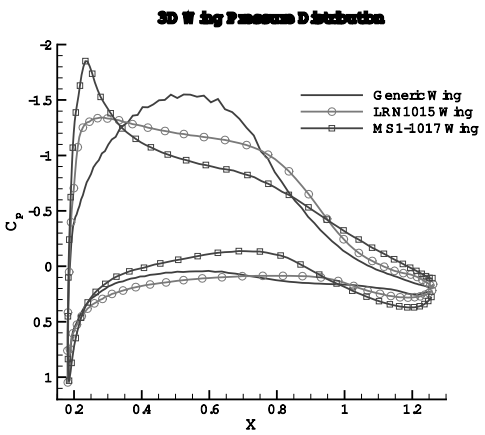

Fig. 9 C_p @ η=0.7 distribution of generic wing

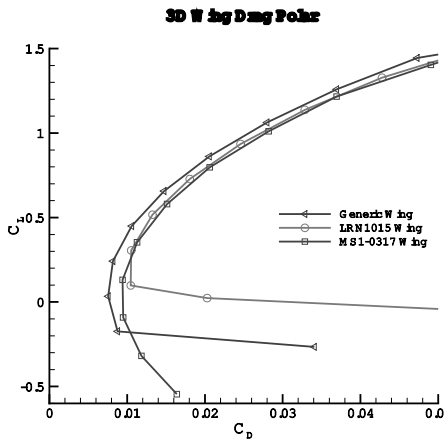

Fig. 10 C_L vs. C_D of generic wing

constructed. To compare the aerodynamic characteristics of several wings, the generic Optimized Min C_d, LRN1015 and MS(1)-0317 wing were analyzed using KFLOW. The grid size for each configuration is 297×41×65 for consistency. Wing has aspect ratio of 20 and leading edge sweep of 1.5°. The flow condition was set to Reynolds number = 2.3×10^6 and Mach number = 0.35.

The sectional C_p's at y/2b = 0.7 of three wings were compared as depicted in Fig. 9. The pressure distributions have smooth pressure recovery on the upper surface. The drag polars were depicted in Fig. 10 which shows that the designed generic wing has better aerodynamic performance compared with other wings. However, aerodynamic performance of 3D flow analysis results is improved less than 2D low Reynolds number analysis. Theses results come from that the present CFD code can't model laminar separation bubbles and flow is assumed to be fully turbulent. The main difficulty of low Reynolds number airfoil design problems is predicting the increase in the profile drag of airfoil that results from laminar separation bubbles.

6. CONCLUSION

In this study, a generic airfoil designed by the inverse method was evaluated with several candidate airfoils using a 2D code which can capture laminar separation bubbles. The baseline generic airfoil and other similar candidate airfoils were optimized by using the couple of optimization formulations to down select the optimum airfoil. After comparing the aerodynamic results, the best airfoil was chosen to construct the baseline 3D wing. A Navier-Stokes code was used to evaluate the overall aerodynamic performance of the designed wing with other wings. The results shows that the designed wing has best aerodynamic performance compared with others. The 3D result was not so promising compared with 2D ones due to incapability of predicting laminar separation bubbles which remains as a future work to be done.

REFERENCES

[1] 1987, Giles, M.B. and Drela, M., "Two Dimensional Transonic Aerodynamic Design Method," *AIAA Journal*, Vol.25, pp.1199-1206.

[2] 1987, Drela, M. and Giles, M.B., "Viscous Inviscid Analysis of Transonic and Low Reynolds Number Airfoils," *AIAA Journal*, Vol.25, pp.1347-1355.

[3] 1985, Drela, M., "Two-Dimensional Transonic Aerodynamic Design and Analysis Using the Euler Equations," Massachusetts Institute of Technology, *PhD Thesis*.

[4] 1989, Drela, M., "XFOIL: An Analysis and Design for Low Reynolds Number Airfoils," *Low Reynolds Number Aerodynamics*, Springer-Verlag.

[5] 1980, Eppler, R. and Somers, D.M., "A Computer Program for the Design and Analysis of Low-Speed Airfoils," *NASA TM80210*.

[6] 1990, Eppler, R., *Airfoil Design and Data*, Springer.

[7] 1998, Drela, M., "Pros & Cons of Airfoil Optimization," *Frontiers of computational fluid dynamics*, World Scientific Publishers.

[8] 2003, Park, S.H. and Kwon, J.H., "On the Dissipation Mechanism of Godunov-type Schemes," *Journal of Computational Physics*, Vol.188, No.2, pp.524-542.
[9] 2003, Kim, Y., Park, S.H., Sung, C.-H. and Kwon, J.H., "Drag Prediction Workshop Results Using the Parallel Multigrid Solver KFLOW3D," *AIAA 2nd Drag Prediction Workshop*, Orlando.
[10] 2004, Park, S.H. and Kwon, J.H., "Implementation of k-ω Turbulence Models in an Implicit Multigrid Method," *AIAA Journal*, Vol.42, 2004, pp.1348-1357.
[11] 1978, Hicks, R.M. and Henne, P.A., "Wing Design By Numerical Optimization," *Journal of Aircraft*, Vol.15, pp.407-412.
[12] 1996, Boggs, P.T. and Tolle, J.W., "Sequential Quadratic Programming," *Acta Numerica*, pp.1-52.
[13] 1989, Maughmer, M.D. and Somers, D.M., "Design and Experimental Results for a High-Altitude, Long Endurance Airfoil," *Journal of Aircraft*, Vol.26, pp.148-153.
[14] 1991, Hicks, R.M. and Cliff, S.E., "An Evaluation of Three Two-Dimensional Computational Fluid Dynamics Codes Including Low Reynolds Numbers and Transonic Mach Numbers," *NASA TM 102840*.